# Detecting the vulnerability of groundwater in semi-confined aquifers using barometric response functions

N.E. Odling [a,*], R. Perulero Serrano [a], M.E.A. Hussein [b], M. Riva [c,d], A. Guadagnini [c,d]

[a] School of Earth and Environment, University of Leeds, Leeds LS2 9JT, UK
[b] AMEC Black Cat LLC, P.O. Box 24523, Doha, Qatar
[c] Politecnico di Milano, Dipartimento di Ingegneria Civile e Ambientale (DICA), Piazza L. Da Vinci, 32, 20133 Milano, Italy
[d] University of Arizona, Department of Hydrology and Water Resources, Tucson, AZ 85721, USA

Received 15 July 2014
Received in revised form 24 October 2014
Accepted 1 November 2014
Available online 11 November 2014

## 1. Introduction

Groundwater vulnerability is an increasingly critical issue for many major aquifers worldwide as water quality regulations (e.g. EU Water Framework Directive) become more stringent, and pressure on existing water resources results in enhanced exploitation of groundwater. In this context, the need to protect aquifers from surface sourced contamination, including agricultural products (e.g. fertilizers, pesticides, fungicides and herbicides) and industrial waste (e.g. hydrocarbon related compounds, radioactive waste, etc.) is becoming increasingly urgent.[1]

### 1.1. Groundwater vulnerability in semi-confined aquifers

Intrinsic vulnerability of an aquifer system is commonly defined as a function of the nature and thickness of the overlying confining layers, the depth to the water table and the characteristics of the aquifer materials (e.g. Boland et al., 1999). Methods for assessing groundwater vulnerability are well established and are under continuous development. In practice, however, the reliability of groundwater vulnerability assessment is limited by quality and

[1] ***BRF*** – barometric response function, ***BE*** – barometric efficiency, ***SBE*** – static barometric efficiency, ***Bp*** – barometric pressure, ***WL*** – borehole water level.

* Corresponding author. Tel.: +44 1133432806.
*E-mail addresses:* n.e.odling@leeds.ac.uk (N.E. Odling), earrser@leeds.ac.uk (R. Perulero Serrano), mahmoud.hussein@amec.com (M.E.A. Hussein), monica.riva@polimi.it (M. Riva), alberto.guadagnini@polimi.it (A. Guadagnini).

quantity of available data, e.g. geological maps, borehole records, geophysical data and estimates of hydraulic conductivity. Assessing groundwater vulnerability of aquifers that are partially protected by heterogeneous semi-confining layers is particularly problematic (Foster, 2007). A particularly common example is aquifers semi-confined by glacial sediments. Large areas of North America, Europe and Eurasia down to 40° N were ice-covered at the Pleistocene Glacial Maximum (Ehlers and Gibbard, 2007) and have an intermittent cover of highly heterogeneous Quaternary glacial sediments ranging from coarse sands and gravels to clays (Johnson and Menzies, 1996). These sediments form semi-confin-ing layers for a number of major aquifers, such as the Cretaceous Chalk and Permian Sandstone Aquifers of North Europe (e.g. Allen et al., 1997; Kilner et al., 2005), the Silurian–Devonian lime-stone aquifers of USA (e.g. Olcott, 1992; Yager, 1996) and the Northern Great Plains Aquifer of Canada (e.g. Vogelsberg, 2007). For such semi-confined aquifers, an appreciation of not only the distribution of sediment types at the land surface but also of the degree to which highly conductive sediment bodies contribute to potential pathways for contaminants from surface to aquifer, is important. The hydraulic conductivity (***K***) of aquifer confining lay-ers at field scale has traditionally been estimated from pumping and slug tests (e.g. Kruseman and de Ridder, 1994). These render predominantly horizontal rather than vertical ***K*** which is most rel-evant to groundwater vulnerability. Estimates of vertical ***K*** of con-fining layers can be obtained from aquifer pumping tests when leakage from the confining layer occurs (e.g. Hantush, 1956). How-ever, to accurately estimate vertical ***K*** from such leakage effects often requires pumping tests performed over time intervals of some tens of hours which are not routinely undertaken for obser-vation boreholes.

The above problems with obtaining good, high quality data for the characterization of confining layer properties limit the accuracy and resolution of groundwater vulnerability assessment. In this context, improved information on the occurrence and location of fully (or partially) penetrating, highly conductive bodies within confining layers that present potential pathways for contaminants would be of value. A key objective of the present work is to explore the use of barometric response functions (***BRFs***) determined from borehole water level (***WL***) and barometric pressure (***Bp***) records in detecting such pathways.

### *1.2. Barometric efficiency and the barometric response function*

That water levels in boreholes tapping confined and semi-confined aquifers respond to barometric pressure is well known (e.g. Jacob, 1940). Fig. 1 shows the aquifer system structure here

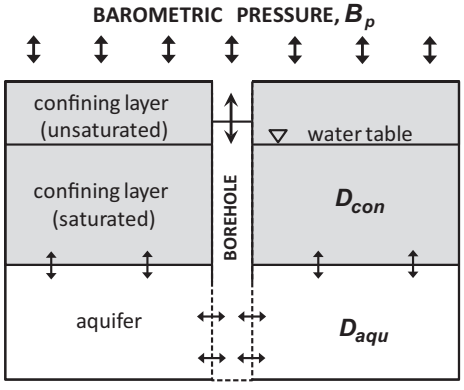


**Fig. 1.** Diagrammatic cross-section showing aquifer, confining layer, borehole and flow directions in response to changing barometric pressure.

considered and the dynamic effects induced by barometric pressure change. In the case of a fully confined aquifer (where the confining layer has negligible hydraulic conductivity), changes in barometric pressure are transmitted virtually instantaneously to the aquifer where they are distributed between the aquifer skeleton and pore waters. The same pressure changes are instantaneously transmitted in total to the water surface in the borehole (e.g. Jacob, 1940; Batu, 1998). This process generates a pressure imbalance between an open borehole and the aquifer so that an increase in barometric pressure causes a decrease in borehole water level and *vice versa.* Where the confining layer is uniformly impermeable, the ratio of change in borehole water level to change in barometric pressure is a constant termed the static barometric efficiency (***SBE***) of the aquifer (Jacob, 1940). The ***SBE*** of an aquifer is related to its elastic properties through specific storage, $S_s$ (Jacob, 1940):

$$\boldsymbol{SBE} = n\beta/(\alpha + n\beta) = \rho g n\beta/\boldsymbol{S_s} \quad (1)$$

where $n$ is formation porosity, $\beta$ is the compressibility of water, $\alpha$ is the compressibility of the aquifer matrix, $\rho$ is the density of water and $g$ is the gravitational constant.

When the aquifer is semi-confined (i.e. where the confining layer has significant permeability) or semi-unconfined (i.e. where there is a thick unsaturated zone and/or an unsaturated zone of low permeability), barometric efficiency (***BE***) becomes frequency dependent (e.g. Weeks, 1979; Furbish, 1991) and the response of borehole water level to barometric pressure is described by a barometric response function (***BRF***). Fig. 2 depicts a typical ***BRF*** in the frequency domain in terms of gain (or ***BE***) and phase (representing the lag of the response). Phase is plotted according of the sign

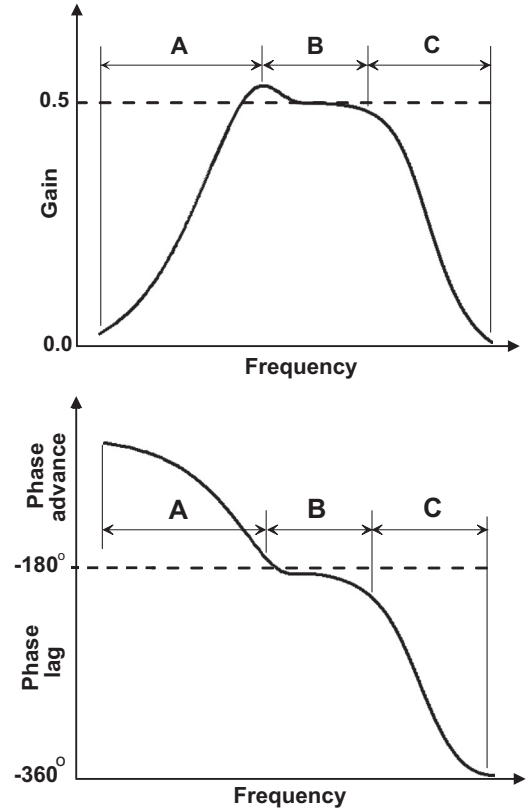


**Fig. 2.** Illustrative barometric response function (top – gain, bottom – phase) showing low (A), intermediate (B) and high (C) frequency response stages. Stage A is controlled largely by the properties of the confining layer, stage B shows behaviour similar to a perfectly confined aquifer with a gain equal to the ***SBE*** of the aquifer and phase of −180°, and stage C is controlled by borehole radius and transmissivity of the aquifer.

convention of Rojstaczer (1988) where phase advance is greater than, and phase lag less than, −180° (which is the lag in the case of a fully confined aquifer where ***BE*** is constant). The ***BRF*** can be divided into the three stages shown in Fig. 2. These comprise low, intermediate and high frequency ranges within the baromet-ric pressure signal (Rojstaczer, 1988; Hussein et al., 2013). At low frequencies (stage A), gain increases and phase decreases with increasing frequency, and the behaviour is controlled primarily by the properties of the confining layer. At very low frequencies, the slow rate of change in barometric pressure allows equilibrium to be maintained between the confining layer, the aquifer and the borehole and the system behaves as if unconfined (gain and phase approach zero). At intermediate frequencies (stage B) a plateau exists at a gain equal to the ***SBE*** and a phase of −180°, showing behaviour resembling that of a fully confined aquifer. At high frequencies (stage C), the ***BRF*** is controlled by the rate at which water can flow in and out of the borehole and therefore by borehole radius and aquifer transmissivity. As a consequence, stage C is associated with decreasing gain and phase with increasing frequency. At very high frequencies, the movement of water cannot keep up with barometric pressure changes and the aquifer once more behaves as if unconfined (gain and phase approach zero).

Barometric response functions can be determined from time series of open borehole water levels and barometric pressure, recorded at regular intervals of around four hours or less for time periods of around one year or more (Hussein et al., 2013). Automatic monitoring of borehole water levels at time intervals of one hour or less is becoming increasingly common so that the often dense networks of monitoring boreholes that exist in many major aquifers can potentially provide ready-made data sets suitable for this approach. Hussein et al. (2013) showed through numerical simulations that the presence of a highly conductive pathway through a confining layer is reflected in the head variation induced by barometric pressure in the aquifer. Here the work of Hussein et al. (2013) is furthered through a study of ***BRFs*** for aquifers with heterogeneous confining layers. Through a suite of numerical simulations, the feasibility of using ***BRFs*** to detect the presence of possible pathways for contaminants within semi-confining layers is investigated and the potential implications for groundwater vulnerability assessment practice are discussed.

### *1.3. Estimating confining layer properties from barometric response functions – previous work*

During the late 1980s and early 1990s, techniques for determining ***BRFs*** from borehole water level and barometric pressure records were established for the time domain (Weeks, 1979; Furbish, 1991; Rasmussen and Crawford, 1997; Rasmussen and Mote, 2007; Toll and Rasmussen, 2007) and the frequency domain (Welch, 1967; Rojstaczer, 1988; Galloway and Rojstaczer, 1988; Rojstaczer and Riley, 1990; Evans et al. 1991) and ***BRFs*** were evaluated for a variety of confined and semi-confined aquifer systems. System properties including vertical diffusivities of confining layers can be estimated from the ***BRF*** through calibration using an appropriate analytical model (e.g. Weeks, 1979; Rojstaczer, 1988; Evans et al., 1991; Butler et al., 2011). Diffusivities estimated com-prise both unsaturated zone pneumatic diffusivity and saturated zone hydraulic diffusivity, the latter defined as the ratio of hydraulic conductivity (***K***) to specific storage ($S_s$) or transmissivity (***T***) to storativity (***S***). For semi-confined aquifers, a number of analytical models for predicting borehole water level response to barometric pressure have been developed both in the time domain (Butler et al., 2011) and in the frequency domain (Hsieh et al., 1987; Rojstaczer, 1988; Evans et al., 1991; Ritizi et al., 1991) and used to estimate confining layer and aquifer properties (Rojstaczer, 1988; Galloway and Rojstaczer, 1988; Rojstaczer and Riley, 1990; Quilty and Roeloffs, 1991; Evans et al., 1991; Beavan et al., 1991; Acworth and Brain, 2008; Butler et al., 2011). ***BRFs*** have also been used to correct borehole water level response for barometric pressure effects (Quilty and Roeloffs, 1991; Rasmussen and Crawford, 1997; Spane, 2002; Toll and Rasmussen, 2007) and the influence of river-stage fluctuations (Spane and Mackley, 2011) where these mask groundwater flow characteristics of interest, e.g. in the estimation of hydraulic gradient or the analysis of pumping test data. The sensitivity of ***BRFs*** to conditions in the immediate vicinity of the borehole (e.g. aquifer transmissivity, borehole radius and skin effects) has been analysed in the time domain by Rasmussen and Crawford (1997) and Spane (2002) and in the frequency domain by Rojstaczer (1988).

***BRFs*** have been used in the past to investigate the degree of aquifer confinement which relates closely to intrinsic aquifer vulnerability. Sensitivity to confinement was demonstrated by Hare and Morse (1997, 1999) for open boreholes within and outside the areal extent of a containment system consisting of a clay cap and impermeable cut-off wall where they used ***BRFs*** as a means of monitoring the performance of the containment system. ***BRFs*** have been used to investigate the continuity of confining layers over distances of up to 700 m (Rasmussen and Crawford, 1997; Butler et al., 2011). Acworth and Brain (2008) demonstrated that a thin weathered zone (<2 metres) in fractured granite can result in a response of borehole water level to barometric pressure indicating confined behaviour and used this response to investigate groundwater-surface water interactions. Hussein et al. (2013) presented ***BRFs*** demonstrating a range in behaviour for an aquifer confined by heterogeneous glacial sediments and related these to groundwater vulnerability. These authors suggested a measure of vulnerability incorporating the thicknesses and diffusivities, estimated from ***BRFs***, of the unsaturated and saturated zones within the confining layer. They also demonstrated, through numerical simulations, that the ***BRF*** reflects the properties of a confining or semi-confining layer over an area extending some hundreds of metres from the monitoring borehole.

## 2. Modelling the impact of high conductivity pathways on barometric response functions

Analytical models that link the ***BRF*** with system properties (e.g. Butler et al., 2011; Hsieh et al., 1987; Rojstaczer, 1988; Evans et al., 1991; Ritizi et al., 1991) assume that both aquifer and confining layer are vertically and laterally homogeneous. In the case where the confining layer is heterogeneous, the properties obtained from these models are interpreted as representative parameters which incorporate the effect of the heterogeneity on the average system behaviour. Of particular interest from the point of view of groundwater vulnerability is the impact on the ***BRF*** of a body of high conductivity material penetrating a low conductivity confining layer. Here the initial work of Hussein et al. (2013) on the influence of a high conductivity pathway within a confining layer is furthered through three-dimensional, transient groundwater flow simulations. The output of the numerical simulations is used to calculate the ***BRF*** for a low conductivity confining layer containing a high conductivity body. These ***BRFs*** are then compared to those generated by the modified analytical model of Rojstaczer (1988) described in Section 2.1, which assumes a homogeneous confining layer, to explore the potential use of ***BRFs*** to detect high flow pathways for contaminants through confining layers.

### *2.1. The analytical model*

Rojstaczer (1988) developed an analytical model in the frequency domain for the response of the water level in an open

borehole to barometric pressure forcing, in a semi-confined aquifer. The model output is the ***BRF*** in terms of gain (***BE***) and phase. Details of the model of Rojstaczer (1988) are given in Appendix A. The model considers three flow processes shown in Fig. 1 that arise from a change in barometric pressure; i) vertical air flow in the unsaturated zone from the Earth's surface to the water table, ii) vertical groundwater flow within the confining layer, and iii) horizontal groundwater flow between the aquifer and the borehole. The model contains nine parameters, i.e. static barometric efficiency of the aquifer (***SBE***), confining layer pneumatic and hydraulic diffusivities ($\boldsymbol{D_{unsat}}$ and $\boldsymbol{D_{con}}$), confining layer thickness ($\boldsymbol{L_{con}}$), unsaturated zone thickness within the confining layer ($\boldsymbol{L_{unsat}}$), aquifer transmissivity ($\boldsymbol{T_{aqu}}$), storativities of the aquifer and confining layer ($\boldsymbol{S_{aqu}}$ and $\boldsymbol{S_{con}}$) and borehole radius ($\boldsymbol{r_w}$).

The frequency dependent fluctuation of the water level in a borehole due to changing barometric pressure is given, as a complex function, by Rojstaczer (1988):

$$x_0 = -A/\rho g + p_0/\rho g - s_0, \tag{2}$$

where $x_0$ is a complex function describing the fluctuation of borehole water level (measured as positive upwards), $p_0$ is a term describing the influence of the confining layer (defined in Eq. (A.2)), and $s_0$ is a term describing the influence of the borehole (defined in Eq. (A.4)). $A$ is the frequency-dependent amplitude of barometric pressure. The first term on the right hand side of (2) governs the amplitude of the water level fluctuations, the second term governs the influence of the confining layer (unsaturated and saturated zones) and the third term, the influence of the borehole on borehole water level fluctuations. The ***BRF*** in term of gain (***BE***) and phase ($\theta$) is then given by:

$$\boldsymbol{BE}(\omega) = |x_0 \rho g/A|, \tag{3a}$$

$$\theta(\omega) = \arg(x_0 \rho g/A), \tag{3b}$$

where $\omega$ is frequency.

In the model of Rojstaczer (1988), propagation of the pressure wave through the saturated confining layer is given by the analytical solution to pressure propagation through a semi-infinite solid, i.e. the pressure at a depth corresponding to the base of the confining layer embedded within a layer of infinite thickness (see Appendix A). This solution represents a simplification of the more rigorous solution comprising pressure propagation in a composite solid of finite thickness (representing the confining layer and aquifer). In the following, the model of Rojstaczer (1988) is revisited and reformulated to incorporate such a composite, finite solid model for the pressure propagation in the saturated confining layer. This is done by adapting the solution for heat conduction in a finite composite solid provided by Carslaw and Jaeger (1959, Section 3.7), as detailed in Appendix A. A comparison between the ***BRFs*** from the original model of Rojstaczer (1988) and the modified model presented here is shown in Fig. 3. These ***BRFs*** are based on the input parameters listed in Table 1, typical for an aquifer with a confined layer composed of glacial sediments. The effect of incorporating a confining layer of finite thickness is seen in the increased steepness of both gain and phase curves at low to intermediate frequencies. These results clearly show that the slope of the curves at low frequencies is dependent on the conceptual model selected for pressure propagation in the confining layer. For most cases, a composite finite, solid model where a confining layer of finite thickness overlies an aquifer of finite thickness is the most appropriate choice. This is the modelling framework employed in this work.

The influence of the borehole and of the saturated and unsaturated zones of the confining layer on the ***BRF*** can be investigated by evaluating separately the contribution of the terms appearing in (2). Fig. 4 shows the analytical solutions, based on the reformulation described above, for the ***BRF*** gain and phase associated with i) the entire system (saturated and unsaturated zones of the confining layer, and borehole of finite radius; solid black curve in Fig. 4), ii) confining layer (saturated and unsaturated zones) only, omitting the influence of the borehole radius (i.e. assuming a borehole of infinitely small radius; dashed grey curve in Fig. 4), and iii) saturated zone of the confining layer alone (i.e. with no unsaturated zone and with a borehole of infinitely small radius; dotted black curve in Fig. 4). Comparing the solid curve with the others in Fig. 4, it can be seen that, for a borehole radius of 0.075 m (typical of monitoring boreholes) or less, the influence of the borehole radius is restricted to high frequencies, above 1 cpd (cycle per day). The influence of the unsaturated zone on the ***BRF*** can be seen to be relatively minor by comparing the dotted and dashed lines in Fig. 4, which differ only by a small reduction in the peak height of the gain curve when the influence of the unsat-urated zone is included.

### 2.2. The numerical model

The effect of the presence of heterogeneities in a confining layer of finite thickness on the ***BRF*** is explored through a suite of numerical simulations, employing MODFLOW 2000 (Harbaugh et al. 2000) in the Visual MODFLOW© environment. The model domain, shown in Fig. 5, is 2 × 4 km in the horizontal plane and 30 m thick. The domain is discretized into a uniform grid with a cell size of 50 × 50 × 2 m. The top ten layers represent a confining layer of 20 m thickness and the lower five layers, an aquifer of 10 m thickness. Barometric pressure is modelled through time dependent hydraulic heads, representing changing barometric pressure, applied to the top layer of the system while all other model boundaries are set to no-flow conditions. Due to the symmetry of the problem, a plane passing through the centre of a single heterogeneity within the confining layer represents a plane across which no flow occurs; thus it is only necessary to model half of the full domain. A region representing half of a high diffusivity heterogeneity with a square horizontal cross-section is placed at the centre of the left hand edge of the model, either fully or partially penetrating the confining layer, as shown in Fig. 5. The confining layer is assigned a uniform hydraulic conductivity and specific storage from a range representative of glacial sediments (clay-rich till, silts and alluvium). The aquifer is assigned a uniform high hydraulic conductivity and low specific storage typical of fractured chalk. The localised heterogeneity in the confining layer is assigned uniform $\boldsymbol{K}$ and $\boldsymbol{S_s}$ values representative of sands and gravels. Table 2 lists all layer properties used in the model.

For simplicity, only pressure changes and flow in the saturated confining layer and aquifer are modelled in this investigation. As discussed above and shown in Fig. 4, the omission of the influence of the unsaturated zone has limited impact on the ***BRF*** for the case studied here. An actual recorded barometric pressure signal from East Yorkshire (UK), expressed as metres of equivalent water head and with the mean removed, is used as a boundary condition for 770 stress periods of 16.75 h duration (total simulation time of c. 537 days). The initial head conditions were set to 0 m through-out the domain and the results associated with the first 20 days of simulations were omitted in the analyses to avoid the influence of the initial conditions. Computed head values were recorded for each stress period through a series of 9 observation boreholes of infinitely small radius screened in the aquifer, placed at a range of distances from the edge of the heterogeneity, as shown in Fig. 5.

***BRFs*** are determined from time series of water level, ***WL***, in each monitoring borehole. Assuming that equilibrium is maintained between borehole and aquifer, ***WL*** is given by:

$$\boldsymbol{WL} = h_{aqu} - B_p, \tag{4}$$

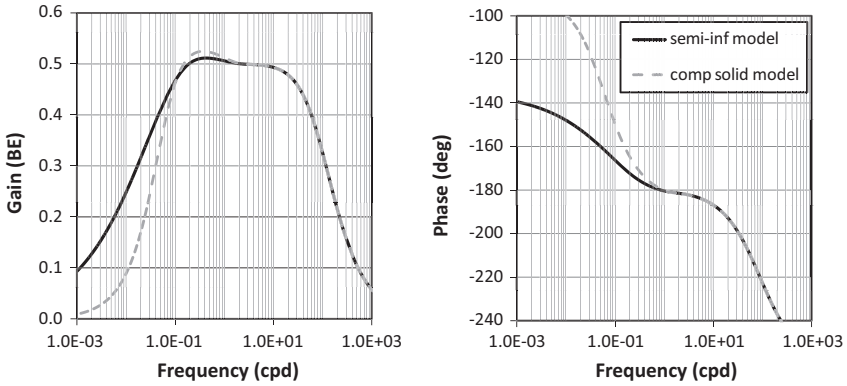


**Fig. 3.** Comparison of ***BRF*** gain (left) and phase (right) curves for the analytical model of Rojstaczer (1988) which employs a semi-infinite solid model for the saturated confining layer (solid black curve), and the modified analytical model which employs a finite, composite layer model for the saturated confining layer and aquifer (dashed grey curve). The modified analytical model results in steeper gain and phase curves at low frequencies.

**Table 1**
Input parameters for Fig. 3.

| Parameter | Value |
|---|---|
| Barometric efficiency, ***BE*** (–) | 0.5 |
| Saturated confining layer thickness, $\boldsymbol{L_{con}}$ (m) | 18 |
| Unsaturated confining layer thickness, $\boldsymbol{L_{unsat}}$ (m) | 2 |
| Confining layer hydraulic diffusivity, $\boldsymbol{D_{con}}$ ($m^2$/d) | 50 |
| Confining layer pneumatic diffusivity, $\boldsymbol{D_{unsat}}$ ($m^2$/d) | 10 |
| Aquifer specific storage, $\boldsymbol{S_{s(aqu)}}$ ($m^{-1}$) | $2.76 \times 10^{-6}$ |
| Confining layer specific storage, $\boldsymbol{S_{s(con)}}$ ($m^{-1}$) | $6.71 \times 10^{-4}$ |
| Well radius, $\boldsymbol{r_w}$ (m) | 0.075 |

where $h_{aqu}$ is the simulated head in the aquifer at the location of the observation borehole and $B_p$ is the barometric pressure (as equivalent water head) at each stress period.

Note that observation boreholes in the numerical model are simply locations at which heads are recorded and are equivalent to boreholes of infinitely small radius. Eq. (4) therefore ignores any storage effects due to exchange of water between borehole and aquifer and thus the influence on the ***BRF*** of finite borehole radius at high frequencies is not modelled. The influence of the borehole radius on the ***BRF*** affects the higher frequencies (Hussein et al., 2013). As shown in Fig. 4, for the borehole radius of 0.075 m (typical for monitoring boreholes) and the aquifer transmissivity used in the numerical model, a finite borehole radius would only influence the ***BRF*** at frequencies greater than 1 cpd.

The numerical model does not include the influence of the elastic properties of the solid aquifer matrix, so that changes in barometric pressure are transmitted in their entirety to aquifer pore waters. Thus, the results are confined to the case of an incompressible aquifer matrix where the static barometric efficiency (***SBE***) equals 1. Here, it is noted that the effect of ***SBE*** on borehole water levels is to scale the magnitude of water level changes induced by barometric pressure. This corresponds to a scaling of the ***BRF*** gain by a factor equivalent to ***SBE*** while the phase remains unaffected (Rojstaczer, 1988; Hussein et al. 2013). ***SBE*** of aquifers covers the range from 0.2 to 0.8 (Batu, 1998). The effects of an ***SBE*** value less than 1 can be represented by simply scaling the changes in borehole water level by ***SBE***, so that the water level in an open borehole (***WL***) is then given by:

$$\boldsymbol{WL} = (h_{aqu} - B_p)\boldsymbol{SBE} \tag{5}$$

In the analysis presented here, a typical ***SBE*** of 0.5 is assumed.

The computed time series of borehole water levels obtained from the numerical model, together with the barometric pressure time series employed as a boundary condition, were then used to determine the ***BRF***. This was accomplished by deconvolving the water level signal by the barometric pressure signal through the technique of cross-spectral deconvolution by ensemble averaging (Welch, 1967), as described by, e.g. Rojstaczer (1988), Rojstaczer and Riley (1990), Beavan et al. (1991), Quilty and Roeloffs (1991) and Hussein et al. (2013). Details of the technique as applied here are given in Hussein et al. (2013) and a brief description is given in

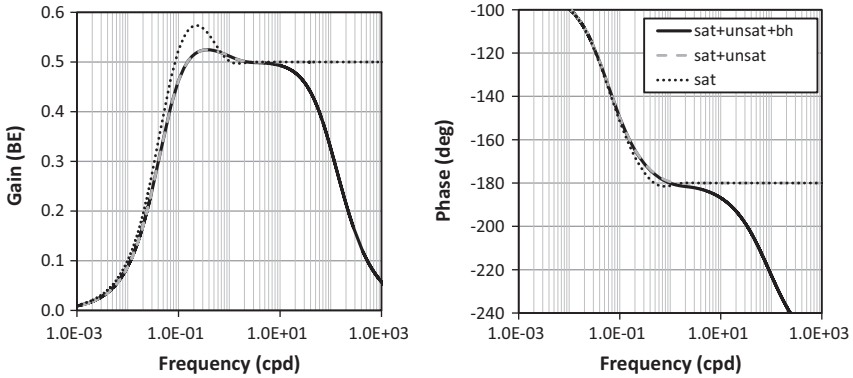


**Fig. 4.** Modified analytical model ***BRF*** curves (left – gain, right – phase) showing the contributions from the confining layer saturated zone only (dotted black curve), the confining layer saturated and unsaturated zones only (dashed grey curve), and the full model comprising confining layer saturated and unsaturated zones, borehole and aquifer transmissivity (solid black curve). The curves show that confining layer saturated and unsaturated zones influence only low frequencies below 1 cpd while the borehole radius and aquifer transmissivity influence only high frequencies above 1 cpd.

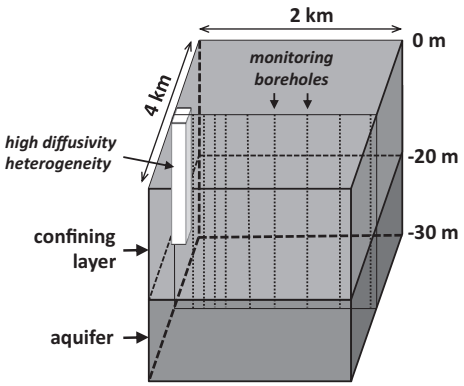


**Fig. 5.** The numerical model showing a confining layer of 20 m thickness containing a high diffusivity heterogeneity, overlying an aquifer of 10 m thickness. A series of monitoring boreholes record head variation with time in the aquifer.

**Table 2**
Input parameters on layer properties for the numerical model (***K*** – hydraulic conductivity, $S_s$ – specific storage, ***D*** – hydraulic diffusivity). ***D*** is the primary model parameter and ***K*** and $S_s$ are chosen to provide the values of ***D*** below.

| Material | ***K*** (m/d) | $S_s$ ($m^{-1}$) | ***D*** ($m^2$/d) |
|---|---|---|---|
| Confining layer A | $1.57 \times 10^{-3}$ | $1.57 \times 10^{-3}$ | 1 |
| Confining layer B | $9.53 \times 10^{-3}$ | $9.53 \times 10^{-4}$ | 10 |
| Confining layer C | $3.35 \times 10^{-2}$ | $6.71 \times 10^{-4}$ | 50 |
| Aquifer | 1 | $2.76 \times 10^{-6}$ | $3.6 \times 10^{5}$ |
| Heterogeneity | 1 | $1.0 \times 10^{-4}$ | $1.0 \times 10^{4}$ |

Appendix B. ***BRFs***, valid over the frequency range 0.017–0.7 cpd, together with one standard deviation error bars for gain and phase, were determined (see Appendix B). This is similar to the frequency range of ***BRFs*** of 0.015 to 0.8 cpd with additional points at 1 and 2 cpd, determined by Hussein et al. (2013) from borehole water level field data. The frequency above which borehole effects are significant (around 1 cpd) lies above the frequency range of the ***BRFs*** calculated in the simulations (0.017–0.7 cpd) so that the lack of an explicitly modelled borehole in the numerical simulations does not affect the results.

## 3. Modelling results

The numerical model was used to determine ***BRFs*** over the frequency range 0.017–0.7 cpd for a series of model scenarios comprising varying confining layer properties and degrees of penetration of a high diffusivity heterogeneity. By determining the best fit analytical model to the numerical model curves, effec-tive parameters (confining layer hydraulic diffusivity and ***BE***) are estimated and compared to numerical model input.

### *3.1. Comparison of numerical and analytical models*

Fig. 6 compares ***BRFs*** derived from the numerical simulations and the corresponding modified analytical models for a homogeneous confining layer. For hydraulic diffusivities of up to 100 $m^2$/d, the ***BRFs*** from the numerical simulations show small error bars and good correspondence with the analytical model. The numerical model curves tend to lie slightly to the right (towards higher frequencies) and, with increasing hydraulic diffusivity, the gain curve peaks become progressively lower than those predicted by the analytical model. For the higher diffusivities of $10^3$ and $10^4$ $m^2$/d, numerical and analytical model results show reasonable correspondence for the gain. However, for the phase, all numerical model curves coincide closely and lie well to the left (towards lower frequencies) of the analytical model curves. Note that the analytical model of Rojstaczer (1988) is specifically for semi-confined aquifers where the confining layer has a significantly lower hydraulic diffusivity than the aquifer, although he does not comment on the range of ratios for aquifer to confining layer hydraulic diffusivity for which his model is valid. In the absence of the influence of the borehole (i.e. when the borehole radius is very small and/or aquifer transmissivity high), the analytical model produces gain curves that approach the ***SBE*** at high frequencies for all values of confining layer hydraulic diffusivity. However, in the case of a truly unconfined aquifer, the gain should be very low at all frequencies (Hussein et al., 2013). The numerical model curves presented here suggest that, for the present set of parameters, the modified analytical model is representative for confining layer hydraulic diffusivities of up to 100 $m^2$/d.

### *3.2. Impact of distance from fully and partially penetrating high diffusivity heterogeneities*

The ***BRFs*** (with one standard deviation error bars) obtained from the numerical simulations for a range of observation borehole distances from a fully penetrating heterogeneity of horizontal dimensions 100 × 100 m are shown in Fig. 7. The most striking feature emerging from these results is that gain decreases with respect to the homogeneous case with decreasing distance between the monitoring borehole and the edge of the heterogene-ity. At locations in the aquifer directly under the heterogeneity itself (i.e. a distance of 0 m), the gain curve is almost flat at a ***BE*** of less than 0.1. The variation with distance from the heterogeneity displayed by the phase curves in Fig. 7 is much less marked than for the gain curves, with only a slight increase in phase seen as the heterogeneity is approached. In all cases, the phase curves lie much closer to the curves for the homogeneous case with the lower confining layer diffusivity than those for the higher heterogeneity diffusivity (see Fig. 7). With increasing distance from the heterogeneity, both gain and phase curves become indistinguishable from those of the homogeneous case. Comparison of the plots for confining layer diffusivities of 1, 10 and 50 $m^2$/d (Fig. 7a–c) shows that the distance at which the ***BRF*** gain and phase curves become indistinguishable from the homogeneous case decreases as confining layer diffusivity increases. Using the one standard deviation error bars as a guide, this distance ranges from 325 m for a confining layer diffusivity of 1 $m^2$/d, to 225 m for a diffusivity of 10 $m^2$/d and 125 m for a diffusivity of 50 $m^2$/d.

Fig. 8 shows the impact on ***BRF*** gain and phase of heterogeneities with horizontal dimensions ranging from 50 × 50 m to 800 × 800 m, for two distances from the heterogeneity edge (25, 125 m). This figure shows that heterogeneity size has a lesser impact on ***BRFs*** than distance from heterogeneity edge. However, increasing heterogeneity size tends to enhance the impact of the heterogeneity on the ***BRF*** with an overall decrease in the gain and increase in the phase as size increases. The impact of heterogeneity size is largest for lowest confining layer hydraulic diffusivity (1 $m^2$/d). At the highest diffusivity of 50 $m^2$/d, heterogeneity size has only a minor effect (Fig. 8c). Similar to Fig. 7, the impact on the gain curves is more marked than on the phase curves.

Fig. 9 shows the impact of high diffusivity heterogeneities of horizontal dimensions 100 × 100 m which fully and partially penetrate the confining layer, for the case of the lowest confining layer diffusivity of 1 $m^2$/d. Two partially penetrating cases, where the heterogeneity penetrates 50% and 90% of the confining layer, were considered. The resulting gain and phase curves are shown for four distances from the heterogeneity edge (0, 25, 125 and 225 m). Fig. 9 reveals that when the heterogeneity penetrates 50% of the confining layer, the ***BRF*** curves are indistinguishable or very close to those for the homogeneous case, even at locations in the aquifer

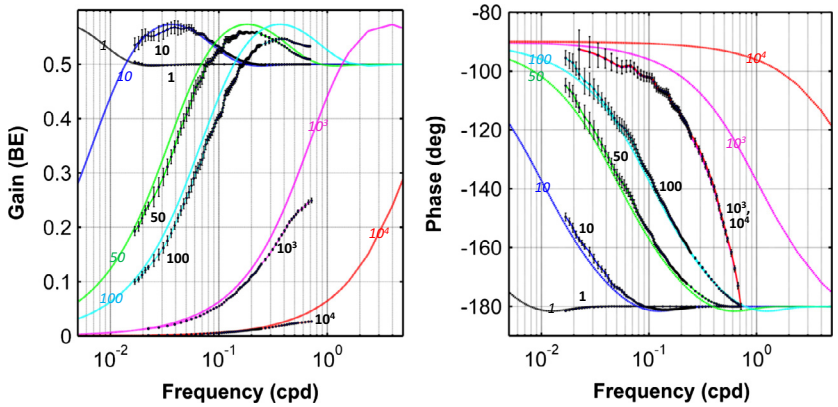


**Fig. 6.** Comparison of barometric response functions (left – gain, right – phase) for the modified analytical model (thick solid curves) and numerical model results (thin solid curves with one standard deviation error bars). Curves are labelled according to their confining layer hydraulic diffusivity ($m^2/d$). The numerical model curves lie slightly to the right but otherwise correspond well to the analytical model curves up to a confining layer hydraulic diffusivity, $\boldsymbol{D_{con}}$, of 100 $m^2/d$.

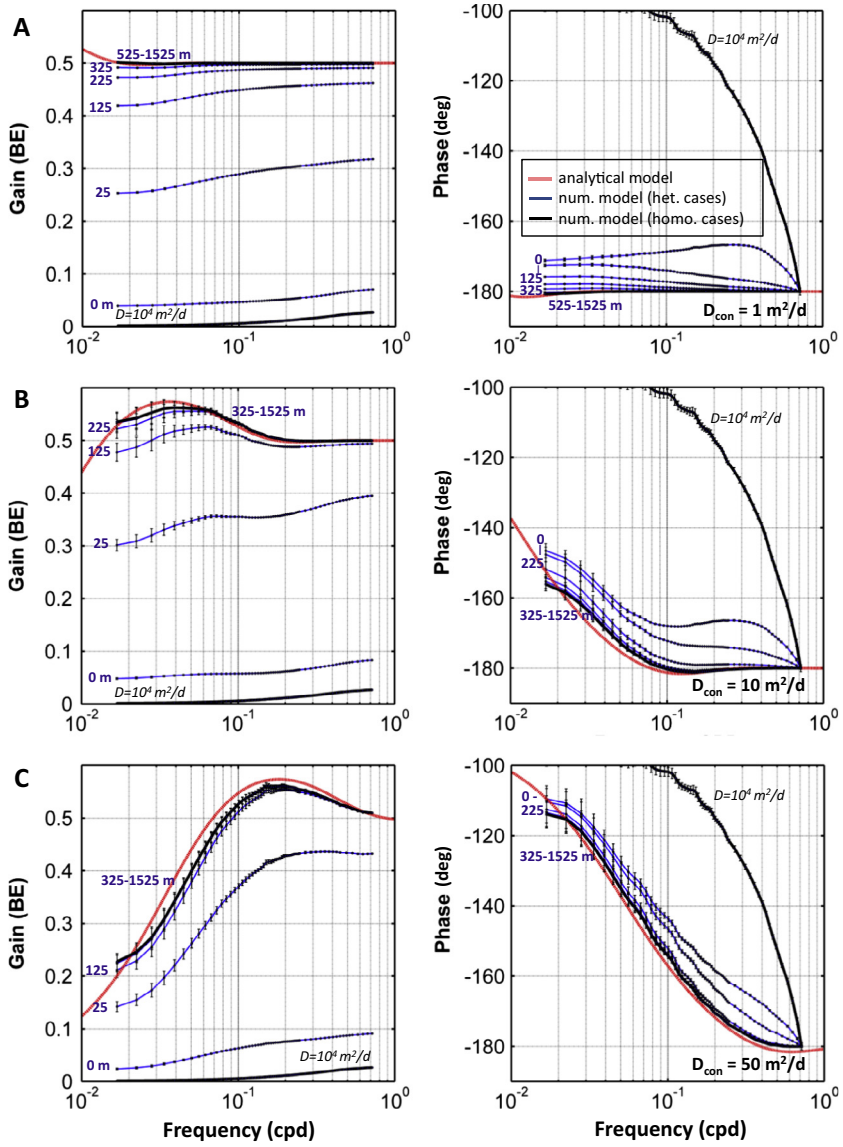


**Fig. 7.** ***BRFs*** from numerical simulations for a fully penetrating heterogeneity (horizontal dimensions 100 × 100 m) of high diffusivity ($10^4$ $m^2/d$) within a confining layer of lower diffusivity (A – 1 $m^2/d$, B – 10 $m^2/d$, C – 50 $m^2/d$). Each pair of plots shows the variation in gain (left) and phase (right) with increasing distance of the monitoring borehole from the edge of a high diffusivity heterogeneity. ***BRFs*** for the homogeneous case with a diffusivity of $10^4$ $m^2/d$ (that of the heterogeneity) are also shown for comparison. Gain curves show marked decrease in gain while phase curves vary to a lesser extent as the heterogeneity is approached. The influence of the heterogeneity is most marked for a low confining layer hydraulic diffusivity (A).

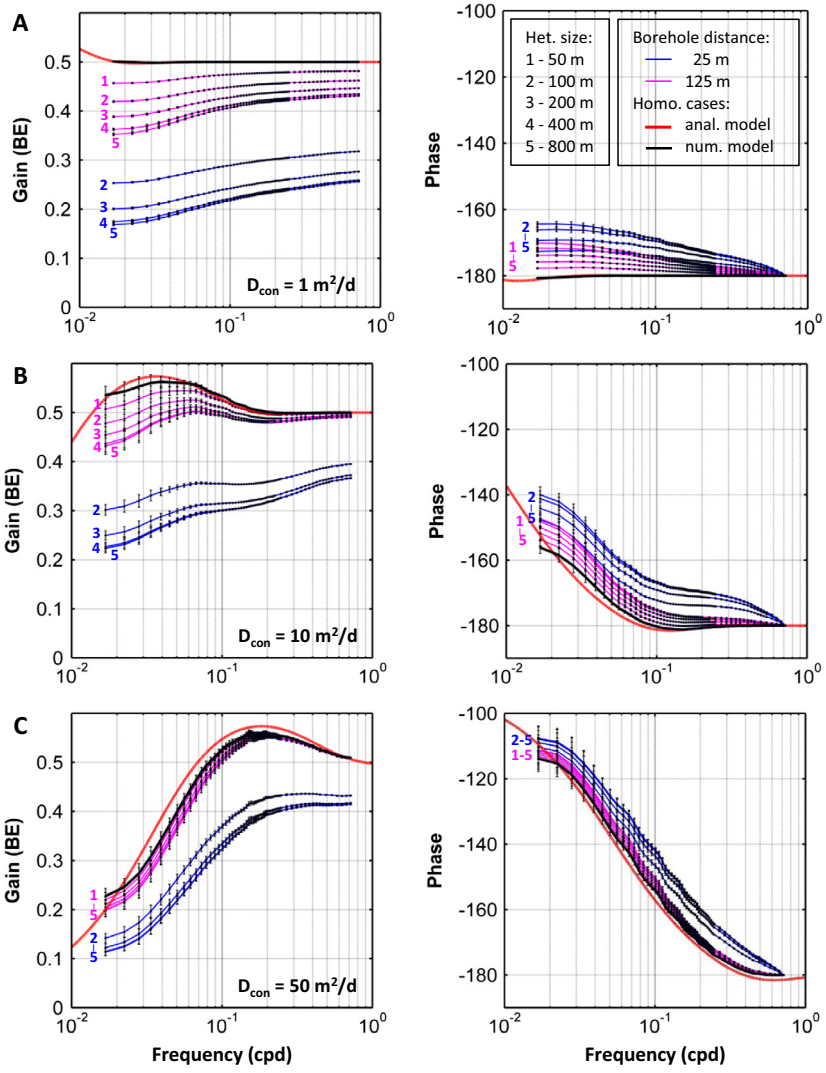


**Fig. 8.** ***BRFs*** from numerical simulations for a fully penetrating heterogeneity of high diffusivity ($10^4$ m$^2$/d) ranging in horizontal dimensions from 50 × 50 m to 800 × 800 m, within a confining layer of lower diffusivity (A – 1 m$^2$/d, B – 10 m$^2$/d, C – 50 m$^2$/d). Sets of curves are shown for two monitoring borehole positions of 25 and 125 m from the heterogeneity edge. Curves for the homogeneous cases (analytical model and numerical simulation ***BRFs***) are shown for comparison. Increasing heterogeneity size slightly increases the influence of the heterogeneity on gain and phase curves, and is most marked for confining layer of low diffusivity (A).

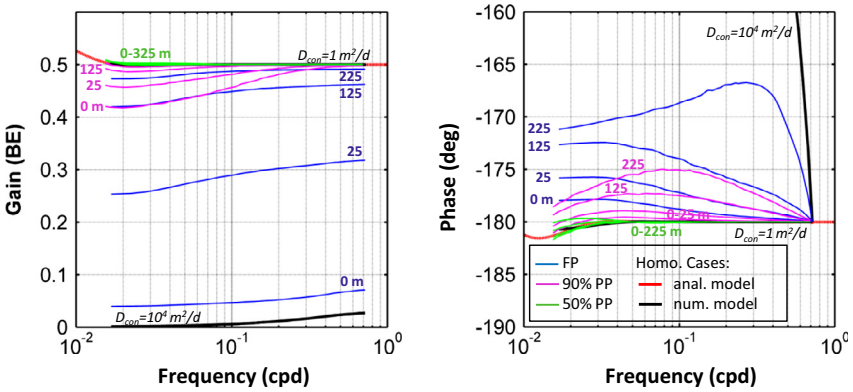


**Fig. 9.** ***BRFs*** from numerical simulations for fully and partially (50%, 90%) penetrating heterogeneities of high diffusivity ($10^4$ m$^2$/d) of horizontal dimensions 100 × 100 m within a confining layer of low diffusivity (1 m$^2$/d). Curves are shown for four monitoring borehole positions at 0, 25, 125 and 225 m from the heterogeneity edge. The influence of the 50% penetrating heterogeneity (50% PP) is negligible, and that of the 90% penetrating heterogeneity (90% PP) limited, compared with the influence of the fully penetrating heterogeneity (FP). The homogeneous case ***BRFs*** from the analytical model (1 m$^2$/d) and numerical simulations ($10^4$ m$^2$/d) are shown for comparison.

directly beneath the heterogeneity. In the case of a 90% penetrating heterogeneity, some influence on the ***BRF*** is detected. However, the effect is significantly less marked than that of a fully penetrating heterogeneity.

### *3.3. Estimating static barometric efficiency and confining layer hydraulic diffusivity*

***SBE*** and confining layer hydraulic diffusivity (***$D_{con}$***) are estimated by fitting the modified analytical model to the ***BRFs*** derived from the numerical simulations. Model calibration is performed using the methodology presented in Hussein et al. (2013) which employs a combined hybrid genetic (GA) and pattern search (PS) algorithm (Alsumait et al., 2010; Liuni et al., 2010). Model parameter estimates are obtained by minimizing the sum of square differences between observed and model ***BRFs*** in the complex plane. Fig. 10 shows the best fit estimates for ***SBE*** and confining layer hydraulic diffusivity (***$D_{con}$***), with their root mean square errors (***RMSEs***) as a function of distance from a fully penetrating heterogeneity of horizontal dimensions 100 × 100 m. As the edge of the heterogeneity is approached, the estimated ***SBE*** reduces by up to a factor of 100 and estimated ***$D_{con}$*** increases by up to a factor of 3 (Fig. 10). ***RMSE*** increases for both gain (by up to a factor of six) and phase (by up to a factor of 60) as the heterogeneity is approached (Fig. 10) and is greatest for the highest confining layer hydraulic diffusivity (50 $m^2$/d). This indicates that when ***BRFs*** are influenced by the presence of a high diffusivity heterogeneity within the confining layer, they deviate increasingly from the ana-lytical model, which assumes a homogeneous confining layer, as the heterogeneity is approached.

The ***BRF*** for an observation borehole in the aquifer beneath the heterogeneity itself would be expected to indicate an unconfined aquifer (gain approaching zero and phase approaching −180°). However, the numerical results show that while the gain is reduced to low values as expected (Fig. 10), the phase remains relatively close to curves appropriate for the lower diffusivity of the bulk of the confining layer (see Fig. 7). Thus, the gain curve largely reflects the diffusivity of the heterogeneity while the phase largely reflects the diffusivity of the bulk of the confining layer. Calibrating the analytical model (where confining layer and aquifer are assumed to be homogeneous) to these results tends to result in estimates for hydraulic diffusivity which reflect the bulk of the confining layer rather than the heterogeneity but with a much reduced ***SBE***, resulting in fits of reduced quality (i.e. larger ***RMSE*** values) as the heterogeneity is approached (Fig. 10).

## 4. Discussion

### *4.1. Detecting high diffusivity pathways using barometric response functions*

The results of the numerical simulations depicted in Figs. 7–10 show that the principal effect on the ***BRF*** of a fully penetrating, high diffusivity heterogeneity within a confining layer is to reduce the gain across all frequencies. This influence diminishes with increasing distance from the heterogeneity edge until the ***BRF*** gain and phase curves approach those of a homogeneous confining layer (Fig. 7). The maximum distance from the monitoring borehole at which the ***BRF*** is significantly influenced by the presence of a high diffusivity heterogeneity is controlled by the hydraulic diffusivity of the bulk of the confining layer. The pressure signal within the aquifer directly beneath the heterogeneity, generated by changing barometric pressure, travels radially outwards from the heterogeneity within the aquifer, becoming attenuated with increasing distance. In addition, the signal may also dissipate through transmission upwards into the confining layer, further enhancing signal attenuation. This latter effect is greater for higher bulk confining layer hydraulic diffusivities. As a consequence, the ***BRF*** is affected by high diffusivity heterogeneities at greater distances from the borehole when the contrast between heterogeneity and confining layer hydraulic diffusivities is large (e.g. a heterogeneity of sands in a confining layer of clay rich tills). For the case of a fully penetrating heterogeneity with horizontal dimensions of 100 × 100 m and a hydraulic diffusivity of $10^4$ $m^2$/d (typical of sands), the maximum distance at which the ***BRF*** is detectably influenced by the heterogeneity ranges from 325 m for a confining layer hydraulic diffusivity of 1 $m^2$/d (typical of clay rich tills) to 125 m for a hydraulic diffusivity of 50 $m^2$/d (typical of silts). Increasing heterogeneity size generally enhances the above effects on the ***BRF***, but has a smaller impact on the ***BRF*** than dis-tance from the heterogeneity. Partially penetrating heterogeneities have virtually negligible impact on the ***BRF***, even when they almost completely penetrate (e.g. 90%) the confining layer. Thus, the ***BRF*** is particularly sensitive to the presence of fully penetrating heterogeneities that form potential pathways for contaminants from the land surface to the aquifer, and could potentially be used to detect the presence of such pathways up to some hundreds of metres from a monitoring borehole.

Estimating system properties by fitting the considered analytical model (which assumes a homogeneous confining layer) to ***BRF*** gain and phase curves influenced by a fully penetrating heterogeneity results in values for ***SBE*** that are much lower than the true

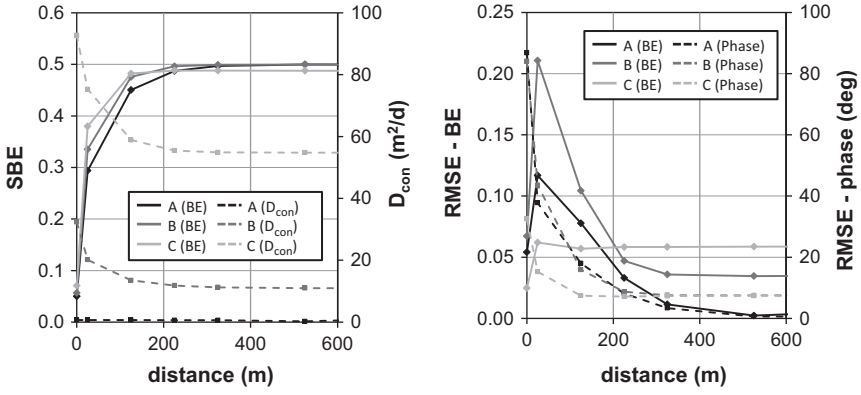


**Fig. 10.** Variation in best fit values of static barometric efficiency, ***SBE***, and confining layer diffusivity, ***$D_{con}$***, with distance from a heterogeneity of horizontal dimensions 100 × 100 m (left), and their ***RMSEs*** (right). The best fit values were obtained by calibrating the modified analytical model to the ***BRFs*** from numerical simulations. Data are shown for three values of confining layer diffusivities; A (1 $m^2$/d), B (10 $m^2$/d), and C (50 $m^2$/d). ***SBE*** decreases, ***$D_{con}$*** increases and all ***RMSEs*** increase as the heterogeneity is approached.

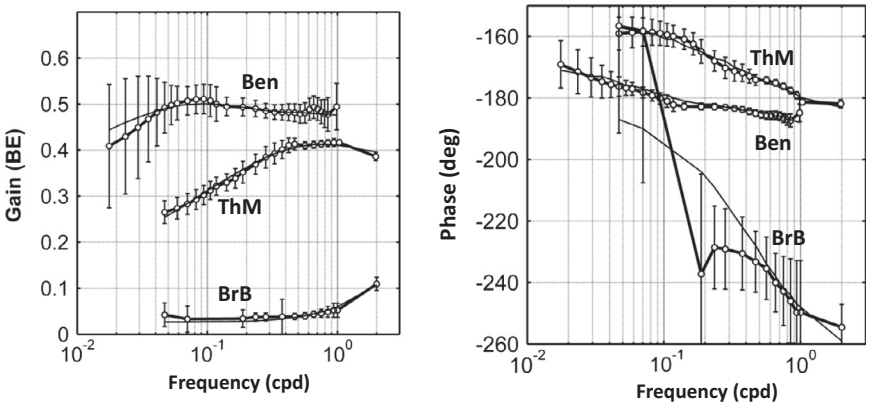


**Fig. 11.** Three ***BRFs*** estimated from water level records belonging to boreholes in the semi-confined Chalk Aquifer of East Yorkshire, UK; Ben – Benningholme, ThM – Thornholme Moor, and BrB – Bracey Bridge boreholes. Thin lines show the best fit analytical model curves for each borehole ***BRF***. The gain and phase curves show a range which corresponds to borehole proximity to glaciofluvial deposits of sands and gravels.

**Table 3**
Borehole details, thickness of confining layer (glacial sediments), water level record length and resulting best fit estimates of ***BE*** and $D_{con}$ determined from ***BRFs***.

| Borehole | | Thickness of glacial sediments (m) | Record length (days) | ***BE*** (–) | $D_{con}$ ($m^2$/d) | ***RMSE*** gain (–) | ***RMSE*** phase (deg) |
|---|---|---|---|---|---|---|---|
| 1. | Benningholme | 16.2 | 799.1 | 0.49 | 10.0 | 0.063 | 6.4 |
| 2. | Thornholme Moor | 19.0 | 312.0 | 0.39 | 310.0 | 0.027 | 5.7 |
| 3. | Bracey Bridge | 9.5 | 309.6 | 0.00 | $2.0 \times 10^4$ | 0.024 | 61.2 |

***SBE*** of the aquifer. Estimates of confining layer hydraulic diffusivity based on the analytical model are likely to more closely reflect the hydraulic diffusivity of the bulk confining layer than the high diffusivity heterogeneity. Only when the borehole is very close (within a few tens of metres) to the edge of the heterogeneity, does the estimated hydraulic diffusivity more closely reflect the high diffusivity heterogeneity. Close to a fully penetrating heterogeneity, the quality of fits of the ***BRF*** to the analytical model also become poorer, being associated with large **RMSE** values. Thus, estimated values of ***SBE*** which are low compared to the expected true ***SBE*** of the aquifer may be indicative of the presence of a fully penetrating high diffusivity heterogeneity within the confining layer in the vicinity (within a few hundred metres) of the borehole. An estimated high hydraulic diffusivity and a poor fit of the ***BRF*** to the analytical model, may indicate the presence of a fully penetrating, high diffusivity heterogeneity very close (within a few tens of metres) to the borehole.

### *4.2. Qualitative comparison of simulation results with field scale evidence*

The results of the numerical modelling study are qualitatively compared to three ***BRFs*** determined for open monitoring boreholes in the semi-confined Chalk Aquifer of East Yorkshire, NE England. This case study aquifer and the determination of two of the ***BRFs*** are presented in detail in Hussein et al. (2013) and brief descriptions are given here, for completeness. The fractured Chalk Aquifer (UK's principal aquifer) in East Yorkshire is semi-confined by Quaternary age, glaciofluvial sediments (Smedley et al., 2004). The confining sediments are up to 50 m thick and are highly heterogeneous, comprising sands and gravels, clay rich till and alluvium. The area is one of intense arable farming and the aquifer is particularly vulnerable to nitrate contamination from agricultural fertilizers (Stuart et al., 2007). Time series of borehole water levels and barometric pressure recorded at 15 min intervals over periods of 294 to 800 days were collected from boreholes in the semi-confined aquifer and ***BRFs*** determined over the frequency range 0.015–2 cpd by the same method to that employed here (Hussein et al., 2013). Confining layer properties were determined by fitting the analytical model of Rojstaczer (1988) to the ***BRFs***. The ***BRFs*** with standard deviation error bars and best fit model curves for three boreholes are shown in Fig. 11. The corresponding best fit values for ***SBE***, hydraulic diffusivity and associated ***RMSEs*** are listed in Table 3.

The gain curves for the Benningholme borehole in Fig. 11 show a typical bell shape and phase that decreases with increasing frequency. The best fit analytical model ***BRF*** curves show a good quality fit (***RMSE*** gain of 0.063, ***RMSE*** phase of 6.4°) yielding an estimated ***SBE*** of 0.49 and confining layer hydraulic diffusivity of 10 $m^2$/d (Table 3), typical of clay rich sediments. This borehole shows one of the highest ***SBE*** values determined from ***BRFs*** in the area (Hussein et al., 2013). Given a compressibility for the Chalk Aquifer matrix in this region of $1.27 \times 10^{-10}$ $Pa^{-1}$ (Bell et al., 1999; Price, 2009) and a matrix porosity of 24.5% (Bell et al., 1999), the ***SBE*** for the aquifer from (1) is 0.48, very close to the ***SBE*** value of 0.49 derived from the ***BRF***. This suggests that the ***SBE*** determined from the ***BRF*** provides a realistic representation of the actual ***SBE*** of the aquifer. It also implies that the confining layer in the vicinity of the borehole (within a radius of around 300 m) has a relatively good spatial continuity and that fully penetrating sediment bodies of high diffusivity are not present. The ***BRFs*** for the boreholes at Thornholme Moor and Bracey Bridge both show overall lower gain and steeper phase curves than those for the Benningholme borehole (Fig. 11). The fit of the analytical model to the ***BRF*** for Thornholme Moor is of good quality (***RMSE*** gain of 0.027 and ***RMSE*** phase of 5.7°), giving a hydraulic diffusivity (310 $m^2$/d) typical of silt-rich alluvium and an ***SBE*** of 0.39, the lat-ter being lower than that estimated for the Benningholme bore-hole. The fit of the analytical model to the ***BRF*** for the borehole at Bracey Bridge is much poorer, particularly for the phase (***RMSE*** gain of 0.024 and ***RMSE*** phase of 61.2°) and gives a very low estimate of ***SBE*** (0.0) and a very high hydraulic diffusivity (20,000 $m^2$/d), typical of sands. By comparing these parameter estimates with the results of the numerical simulations illustrated in Section 3, it is

possible to infer that the lower estimates for ***SBE*** and larger hydraulic diffusivities for the boreholes at Thorneholme Moor and Bracey Bridge may be associated with the occurrence of one or more fully penetrating high diffusivity pathways that lie within 200 to 300 m of these boreholes. The very high value of hydraulic diffusivity at Bracey Bridge and the poor fit by the analytical model suggest that this borehole lies very close to a fully penetrating heterogeneity of high diffusivity.

The borehole logs of all three boreholes show considerable proportions of clay-rich material in the glacial sediments overlying the aquifer (Benningholme 42%, Thornholme Moor 84% and Bracey Bridge 93%). This suggests very low confining layer hydraulic diffusivities which are in contrast to estimates of hydraulic diffusivity from the ***BRFs*** at Thorneholme Moor and Bracey Bridge (310 and 20,000 $m^2/d$, respectively). Geological maps of the glacial sediments in the vicinity of these boreholes indicate that while the borehole at Benningholme lies within outcropping alluvium surrounded by glacial till, the boreholes at both Thornholme Moor and Bracey Bridge lie close (70 and 20 m, respectively) to outcropping glacial sands and gravels. The geological maps are therefore consistent with the conclusion from the ***BRFs*** that the boreholes at Thornholme Moor and Bracey Bridge lie close to fully penetrating, high diffusivity heterogeneities whereas the borehole at Benningholme does not. The ***BRFs*** for Thornholme Moor and Bracey Bridge also indicate that the nearby outcropping bodies of sands and gravel fully penetrate the confining layer, something that cannot be deduced from the geological map alone. The ***BRFs*** for these three boreholes therefore suggest low aquifer vulnerability, reflecting a relatively continuous low diffusivity confining layer, in the vicinity of the Benningholme bore-hole and high aquifer vulnerability, due to high diffusivity fully penetrating heterogeneities in the confining layer, in the vicinity of the Thornholme Moor and Bracey Bridge boreholes.

### *4.3. Potential contribution to groundwater vulnerability assessment in practice*

In the numerical simulations, the sole influence on borehole water levels is barometric pressure, and standard error bars for the ***BRFs*** are small (Figs. 7–9). In practical field conditions, borehole water level records are also influenced by other forcing terms such as recharge, Earth tides and pumping. Although it is possible to remove some of these influences (e.g. Earth tides, Rasmussen and Mote, 2007), the errors typically associated with ***BRFs*** determined from borehole water level records are in practice much larger than those derived from the numerical simulations presented here. These effects will tend to reduce the distance from an observation borehole at which the occurrence of a high diffusivity heterogeneity can be reliably detected. The joint analysis of the numerical simulation results of Section 3 and the field case study presented in Section 4.2, however, strongly suggests that ***BRFs*** can indeed be used to detect the presence of high diffusivity path-ways in heterogeneous confining layers in real cases.

The numerical simulations and the field case study suggest that ***BRFs*** estimated from monitoring borehole records may be used to detect the presence of high diffusivity pathways through a confining layer up to a distance of a few hundred metres from the borehole. The distance between monitoring boreholes is, however, typically around one or more kilometres. For instance, in the Chalk Aquifer of East Yorkshire, UK, the spacing between monitoring boreholes ranges from 700 m to 3 km in areas with dense coverage to around 5 to 10 km in more sparsely monitored areas. At this density of monitoring boreholes, ***BRFs*** cannot be reliably used to detect all existing high diffusivity pathways. However, ***BRFs*** determined from a number of monitoring boreholes could be useful in assessing the variation in aquifer confinement across the region. For example, if estimated ***BRFs*** from a specific aquifer system show a wide range of behaviours with, in particular, estimates of ***SBE*** values significantly lower than the expected true ***SBE*** of the aquifer, this could indicate the presence of fully penetrating high diffusivity pathways within the confining layer. The characteristics of the ***BRFs*** could then be used together with available geological maps of confining layer lithology to gauge the likelihood that outcropping deposits of high diffusivity material (such as sands and gravels) form potential pathways for contaminants.

An additional factor in the potential application of ***BRFs*** in aquifer vulnerability is that much manual monitoring of borehole water levels at monthly (or less frequent) intervals has in recent years been replaced by automatic monitoring using pressure transducers recording at hourly (or more frequent) intervals. Barometric pressure is routinely recorded by weather stations at 15 min or hourly intervals. Therefore there is a growing body of borehole water level data recorded from open monitoring boreholes for most major aquifers which could be used to estimate ***BRFs***. The likelihood of potential high diffusivity pathways through confining layers derived from ***BRFs*** could then be combined with information such as seasonal head gradient directions, as well as spatial and temporal variation in the chemical loading (such as fertilizers and pesticides) to improve aquifer vulnerability assessment. In addition, these techniques could be used as a basis for establishing additional monitoring boreholes in areas of especially high risk such as groundwater abstraction well protection zones; thus contributing to more effectively targeted policies on, e.g. agrochemical usage and industrial development.

## 5. Conclusions

Past studies have shown that barometric response functions determined from borehole water level and barometric pressure data can be used to estimate confining layer hydraulic diffusivity through calibration by an analytical model (e.g. Rojstaczer, 1988). Available analytical models treat the confining layer as a homogeneous unit, an assumption which, in many semi-confined aquifers, is not realistic. In this study, numerical simulations have been used to investigate the potential of ***BRFs*** in detecting the presence of fully penetrating, high diffusivity heterogeneities within otherwise low diffusivity confining layers that represent potential pathways for contamination to the aquifer. The system behaviour revealed through the analysis of numerical simulations has then been employed to interpret observed field scale ***BRFs***. The study leads to the following major conclusions.

- In the analytical model of Rojstaczer (1988), the solution used for pressure propagation in the saturated confining layer controls the slope of the ***BRF*** gain and phase curves at low frequencies. A modified model incorporating the solution for pressure propagation in a finite, composite (two-layer) model was found to be more appropriate than the original model in which a solution for a semi-infinite solid was assumed.
- Numerical simulations show that the impact on the ***BRF*** of a fully penetrating, high diffusivity heterogeneity within an otherwise low diffusivity confining layer decreases, and approaches the homogeneous case, with increasing distance from the heterogeneity. The key effect of the heterogeneity is the reduction of the ***BRF*** gain, with limited effect on the phase.
- Effective parameters obtained by fitting the modified analytical model to ***BRFs*** derived from numerical simulations show a marked reduction in ***SBE*** with respect to the true ***SBE*** of the aquifer, as the monitoring borehole location approaches a high diffusivity heterogeneity.
- The maximum distance at which a high diffusivity, fully penetrating heterogeneity can be detected is greatest when the bulk confining layer hydraulic diffusivity is low. The numerical

simulations indicate that this detection distance ranges from 325 m for a confining layer diffusivity of 1 $m^2$/d (e.g. clay-rich tills), to 225 m for a diffusivity of 10 $m^2$/d (e.g. silts) and 125 m for a diffusivity of 50 $m^2$/d (e.g. silts and fine sands). In practice, however, ***BRFs*** determined from real borehole water level data have larger errors which will tend to reduce these detection distances.
- Increasing heterogeneity size enhances the effect on the ***BRF*** but is of secondary importance to distance of the monitoring borehole to the heterogeneity.
- Partially penetrating heterogeneities have little impact on the ***BRF***.
- ***BRFs*** from borehole water level data from the semi-confined Chalk Aquifer in East Yorkshire, NE England, confirm that ***BRFs*** may be used to detect high diffusivity pathways through confining layers in practical applications. The ***BRFs*** give information on the vertical continuity of high diffusivity material within confining layers, information that cannot be deduced from geological maps alone.
- An increase in automated monitoring of borehole water levels is nowadays generating data sets suitable for estimating ***BRFs***. Although aquifer monitoring borehole coverage will seldom be sufficient to allow all high diffusivity pathways to be detected, the range in ***BRFs*** estimated from borehole records across a semi-confined aquifer could be used to assess the continuity likelihood of low diffusivity lithologies within confining layers. This could then make a significant contribution to groundwater vulnerability assessment and also form the basis for further targeted studies in high risk areas such as abstraction well protection zones.


## Acknowledgements

This research was supported by funding under the EU Marie Curie Initital Training network scheme (PITN-GA-2008-212298), the University of Leeds (UK), and Politecnico di Milano (Italy).


## Appendix A. Theoretical barometric response functions – the analytical model of Rojstaczer (1988) and modifications

### *A.1. The analytical model of Rojstaczer (1988)*

An analytical model for the barometric response function reflecting water level change in an open borehole tapping a semi-confined aquifer due to barometric pressure change is given by Rojstaczer (1988). In this model, the frequency dependent fluctuation of the water level in the borehole due to changing barometric pressure is given by:

$$x_0 = -A/\rho g + p_0/\rho g - s_0, \tag{A.1}$$

where $x_0$ is a complex function describing the fluctuation of the water level (measured as positive upwards), $p_0$ is a term describing the influence of the confining layer and $s_0$ is a term describing the influence of the borehole. $A$ is the frequency dependent amplitude of barometric pressure, $\rho$ is the density of water and $g$ is the gravitational constant. The first term on the right hand side of (A.1) governs the amplitude, the second term, the influence of the confining layer (unsaturated and saturated zones) and the third term, the influence of the borehole. The parameter $p_0$ in (A.1) is given by:

$$p_0 = A((M + iN - \gamma)\exp(-(i+1)\sqrt{Q}) + \gamma), \tag{A.2}$$

Here, $i$ is the complex number; $\gamma = (1 - \textbf{\textit{BE}})$ is the loading efficiency of the aquifer where ***BE*** is the barometric efficiency; and $Q = L_{con}^2\omega/2D$ where $D$ is the hydraulic diffusivity of the confining layer saturated zone, $L_{con}$ is the confining layer thickness and $\omega$ is frequency. The propagation of the pressure wave through the confining layer is given by the solution to pressure propagation through a semi-infinite solid, described by the term $[\exp[-(i+1)\sqrt{Q}]]$ in (A.2). The quantities $M$ and $N$ in (A.2) are given by:

$$M = \frac{2\cosh(\sqrt{R})\cos(\sqrt{R})}{\cosh(2\sqrt{R}) + \cos(2\sqrt{R})} \tag{A.3a}$$

$$N = \frac{2\sinh(\sqrt{R})\sin(\sqrt{R})}{\cosh(2\sqrt{R}) + \cos(2\sqrt{R})}, \tag{A.3b}$$

where $R = L_{unsat}^2\omega/2D_a$, and $D_a$ and $L_{unsat}$ are, respectively, the pneumatic diffusivity of the confining layer unsaturated zone and the unsaturated zone thickness. The parameter $s_0$ in (A.1) is given by:

$$s_0 = i\ 0.5Wx_0K_0(W^2(S^2 + 1/q^2))^{0.25} \cdot \exp(i\ 0.5(\tan^{-1}(qS))). \tag{A.4}$$

Here, $K_0$ is the modified Bessel function, $W = \omega r_w^2/T$, $q = L_{con}\omega/K_{con} = 2Q/S$ where $r_w$ is the radius of the borehole, $T$ is aquifer transmissivity, $K_{con}$ is the confining layer hydraulic conductivity, and $S$ is the storage coefficient of the aquifer and confining layer.

The barometric response function in terms of gain, ***BE***$(\omega)$ and phase, $\theta(\omega)$ is then given by:

$$\textbf{\textit{BE}}(\omega) = |x_0\rho g/A|, \tag{A.5a}$$

$$\theta(\omega) = \arg(x_0\rho g/A). \tag{A.5b}$$

where arg denotes the inverse tangent of the ratio of the imaginary to real parts of the complex function.

### *A.2. Modifications to the analytical model of Rojstaczer (1988)*

In the modification of the model of Rojstaczer (1988), the solution for pressure propagation through the saturated confining layer, which in Rojstaczer's model (A.2) is that of pressure propagation in a semi-infinite solid, is replaced with the solution for pres-sure propagation in a finite composite solid representing the confining layer and the aquifer, according to the conceptual picture shown in Fig. A.1.

The solution to heat conductance in a solid composed of two layers with differing properties and periodic surface temperature is given by Carslaw and Jaeger (1959, section 3.7). This is modified for pressure propagation in a saturated medium by substituting

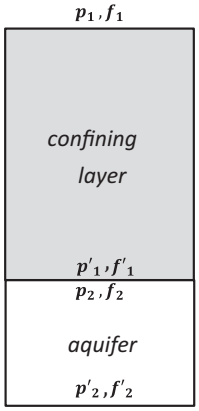


**Fig. A.1.** Cross-section through a solid composed of two layers (confining layer – layer 1 and aquifer – layer 2) with pressures and fluxes at the upper ($p_1$, $f_1$, $p_2$, $f_2$) and lower ($p'_1$, $f'_1$, $p'_2$, $f'_2$) boundaries of each layer.

pressure for temperature and hydraulic diffusivity for thermal diffusivity to give:

$$\begin{pmatrix} p'_2 \\ f'_2 \end{pmatrix} = \begin{pmatrix} A_1A_2 + B_1C_2 & A_1B_2 + B_1D_2 \\ C_1A_2 + D_1C_2 & C_1B_2 + D_1D_2 \end{pmatrix} \cdot \begin{pmatrix} p_1 \\ f_2 \end{pmatrix} \cdot \exp(i\omega t), \quad \text{(A.6)}$$

where $p_n$ is the pressure and $f_n$ is the flux at the upper face, and $p'_n$ and $f'_n$ are, respectively, pressure and flux at the lower face of the $n$th layer, and:

$$A_n = \cosh\left(\sqrt{Q_n}(1+i)\right),$$

$$B_n = \sinh\left(\sqrt{Q_n}(1+i)\right) / \left(K_n \frac{\sqrt{Q_n}}{L_n}(1+i)\right),$$

$$C_n = -K \frac{\sqrt{Q_n}}{L_n}(1+i)\sinh(\sqrt{Q_n}(1+i)),$$

$$D_n = \cosh(\sqrt{Q_n}(1+i)). \quad \text{(A.7)}$$

Here, $n = 1$ is the confining layer and $n = 2$ is the aquifer, $L_n$ is the thickness of the $n$th layer, and $Q_n = L_n^2\omega/2D_n$ where $D_n$ is the hydraulic diffusivity of the $n$th layer. The required quantity for the evaluation of the analytical model (Rojstaczer, 1988) is the pres-sure condition at the base of layer 1 (the confining layer), $p'_1 = p_2$.

Flux, $f'_2$, across the base of the aquifer is assumed to be zero (a no-flow boundary). The pressure at the base of the aquifer is the obtained from (A.6) as:

$$p'_2 = [(A_2A_1 + B_2C_1)p_1 + (A_2B_1 + B_2D_1)f_1] \cdot \exp(i\omega t), \quad \text{(A.8a)}$$

$$f'_2 = [(A_1C_2 + D_2C_1)p_1 + (C_2B_1 + D_2D_1)f_1] \cdot \exp(i\omega t) = 0 \quad \text{(A.8b)}$$

thus:

$$f_1 = p_1[(A_1C_2 + D_2C_1)/(C_2B_1 + D_2D_1)], \quad \text{(A.9)}$$

where $p_1$ is the amplitude of the input barometric input signal.

Following Carslaw and Jaeger (1959, section 3.7), the relationship between pressure and flux at the top and bottom of the confining layer (layer 1) is:

$$\begin{pmatrix} p'_1 \\ f'_1 \end{pmatrix} = \begin{pmatrix} A_1 & B_1 \\ C_1 & D_1 \end{pmatrix} \cdot \begin{pmatrix} p_1 \\ f_1 \end{pmatrix} \cdot \exp(i\omega t) \quad \text{(A.10)}$$

and so the pressure at the base of the confining layer, $p'_1$, is:

$$p'_1 = A_1p_1 + B_1f_1. \quad \text{(A.11)}$$

Now substituting for $f_1$ allows (A.11) to be rewritten as:

$$p'_1 = p_1\left[A_1 - B_1\frac{(A_1C_2 + D_2C_1)}{(C_2B_1 + D_2D_1}\right]. \quad \text{(A.12)}$$

Using (A.12) for the pressure at the base of the confining layer and substituting (A.12) into (A.2) yields:

$$p_0 = p/A\exp(i\omega t) = \left[[M + iN - \gamma] \cdot \left[A_1 - B_1\frac{(A_1C_2 + D_2C_1)}{(C_2B_1 + D_2D_1)}\right] + \gamma\right], \quad \text{(A.13)}$$

where $p$ is the pressure at the base of the saturated confining layer.

## Appendix B. Brief description of the determination of the *BRF* from water level and barometric pressure records

The barometric response function (***BRF***) is determined from borehole water level and barometric pressure time series by deconvolving the water level signal by the barometric pressure signal through the technique of cross-spectral deconvolution by ensemble averaging (Welch, 1967). This technique is described and applied in Rojstaczer (1988), Rojstaczer and Riley (1990), Beavan et al. (1991), Quilty and Roeloffs (1991) and Hussein et al. (2013). Details of the technique as applied here are given in Hussein et al. (2013) and only a brief description is given below.

In this technique, a number of partially independent barometric response functions are determined from overlapping segments of the water level and barometric pressure-signals (Bendat and Piersol, 2010). This technique is applied to five overlapping frequency bands, each with its own number of segments, $N$, according to the method of Beavan et al. (1991). To obtain values of the ***BRF*** in the lowest frequency band, a small number of segments must be used to maximise segment length, resulting in lower accuracy and larger error bars. For high frequency bands, a larger number of segments can be used resulting in greater accuracy and smaller error bars. The results for each set of segments are then averaged to give the final barometric response function with one standard deviation errors. This procedure optimizes accuracy and smooths the ***BRF***.

Barometric response functions were determined using the MATLAB© codes provided as supplementary information in Hussein et al. (2013). Before determining the barometric response function, the first 20 days of water level and barometric pressure data were omitted to avoid the influence of the initial conditions in the numerical simulations, leaving time series for borehole water level and barometric pressure of 517 days duration. The signals were then detrended (linear trend is removed and mean sub-tracted). Eighteen segments with an overlap of 0.5 were used for the lowest frequency band in the ***BRF***. The lowest theoretically valid frequency in the barometric response function is given by the inverse of the largest segment length (here 117 days) divided by segment overlap (here 0.5 days), giving 0.017 cpd. The highest theoretically valid frequency in the barometric response function is around 70% of the Nyquist frequency which is equal to the inverse of twice the recording time interval (Gubbins, 2004). With the recording interval used in the numerical simulations of 16.75 h, this gives a maximum frequency of 0.72 cpd. Barometric response functions are therefore determined for the range 0.017–0.7 cpd.

## References


Acworth, R.I., Brain, T., 2008. Calculation of barometric efficiency in shallow piezometers using water levels, atmospheric and Earth tide data. Hydrogeol. J. 16 (8), 1469–1481.

Allen, D.J., Bloomfield, J.P., Robinson, V.K., 1997. The physical properties of major aquifers in England and Wales. Technical Report (British Geological Survey) WD/97/34, Environment Agency R&D Report 8, 312 pp. Published BSG, Nottingham, UK.

Alsumait, J.S., Sykulski, J.K., Al-Othman, A.K., 2010. A hybrid GAPS-SQP method to solve power system valve-point economic dispatch problems. Appl. Energy 87, 1773–1781.

Batu, V., 1998. Aquifer Hydraulics; A Comprehensive Guide to Hydrogeologic Data Analysis. John Wiley & Sons Inc., New York, N.Y..

Bendat, J.S., Piersol, A.G., 2010. Random Data Analysis and Measurements Procedures. John Wiley & Sons Inc., New York, N.Y..

Beavan, J., Evans, K., Simpson, S., Mousa, D., 1991. Estimating aquifer parameters from analysis of forced fluctuations in well level: an example from the Nubian formation near Aswan, Egypt. 2. Poroelastic properties. J. Geophys. Res-Solid 96 (B7), 12139–12160.

Bell, F.G., Culshaw, M.G., Cripps, J.C., 1999. A review of selected engineering geological characteristics of English Chalk. Eng. Geol. 54, 237–269.

Boland, M.P., Klinck, B.A., Robins, N.S., Stuart, M.E., Whitehead, E.J., 1999. Guidelines and Protocols for investigations to assess site specific groundwater vulnerability, Rep. R&D Project Record P2/042/01, Environment Agency, UK.

Butler Jr., J.J., Jin, W., Mohammed, G.A., Reboulet, E.C., 2011. New insights from well responses to fluctuations in barometric pressure. Ground Water 49 (4), 525–533. http://dx.doi.org/10.1111/j.1745-6584.2010.00768.x.

Carslaw, H.S., Jaeger, J.C., 1959. Conduction of Heat in Solids. Oxford Science Publications.

Ehlers, J., Gibbard, P.L., 2007. The extent and chronology of Cenozoic global glaciation. Quatern. Int. 164–165, 6–20.

Evans, K., Beavan, J., Simpson, D., Mousa, S., 1991. Estimating aquifer parameters from analysis of forced fluctuations in well level: an example from the Nubian formation near Aswan, Egypt. 3. Diffusivity estimates for saturated and unsaturated zones. J. Geophys. Res-Solid 96 (B7), 12161–12191.

Foster, S., 2007. Aquifer pollution vulnerability concept and tools – use, benefits and constraints. In: Witkowski, A.J., Kowalczyk, A., Vrba, J. (Eds.), Groundwater Vulnerability Assessment and Mapping. IAH Selected Papers on Hydrology, vol. 11. Taylor and Francis, London, pp. 3–9.

Furbish, D.J., 1991. The response of water level in a well to a time series of atmospheric loading under confined conditions. Water Resour. Res. 27 (4), 557–568.

Galloway, D., Rojstaczer, S., 1988. Analysis of the frequency response of water levels in wells to Earth tides and Atmospheric loading. Paper presented at 4th Canadian/American conference, vol. 4, pp. 100–113.

Gubbins, D., 2004. Time Series Analysis and Inverse Theory for Geophysicists. Cambridge Univ. Press, Edinburgh, UK.

Hantush, M.S., 1956. Analysis of data from pumping tests in leaky aquifers. Trans. Amer. Geophys. Union 37, 702–714.

Harbaugh, A.W., Banta, E.R., Hill, M.C., McDonald., M.G., 2000. MODFLOW-2000, the U.S. Geological Survey modular ground-water model user guide to modularization concepts and the ground-water flow process. U.S.G.S., Open-File Report 00-92, p. 127.

Hare, P.W., Morse, R.E., 1997. Water-level fluctuations due to barometric pressure changes in an isolated portion of an unconfined aquifer. Ground Water 35 (4), 667–671.

Hare, P.W., Morse, R.E., 1999. Monitoring the hydraulic performance of a containment system with significant barometric pressure effects. Ground Water 37 (5), 755–763.

Hsieh, P.A., Bredehoeft, J.D., Farr, J.M., 1987. Determination of aquifer transmissivity from Earth tide analysis. Water Resour. Res. 23 (10), 1824–1832. http://dx.doi.org/10.1029/WR023i010p01824.

Hussein, M.E.A., Odling, N.E., Clark, R.A., 2013. Borehole water level response to barometric pressure as an indicator of aquifer vulnerability. Water Resour. Res. 49, 7102–7119. http://dx.doi.org/10.1002/2013WR014134.

Jacob, C.E., 1940. The flow of water in an elastic artesian aquifer. Eos Trans., AGU 21, 574–586.

Johnson, W.H., Menzies, J., 1996. Pleistocene supraglacial and ice-marginal deposits and landforms. In: Menzies, J. (Ed.), Past Glacial Environments, Sediments, Forms and Techniques. Martins the Printers Ltd., UK.

Kilner, M.D., West, L.J., Murray, T., 2005. Characterization of glacial sediments using geophysical methods for ground source protection. J. Appl. Geophys. 57, 293–305. http://dx.doi.org/10.1016/j.jappgeo.2005.02.002.

Kruseman, G.P., De Ridder, N.A., 1994. Analysis and Evaluation of Pumping Test Data, second ed. Int. Inst. for Land Reclam. and Impr, Wageningen, Netherlands.

Liuni, M.P., Loddo, M., Schiavone, D., 2010. Non-linear Inversion using a Hybrid Global Search Algorithm: Applications in Gravimetry, Extended abstract, presented at EGM 2010 International Workshop, April 11–14, Adding new value to Electromagnetic, Gravity and Magnetic Methods for Exploration, Capri, Italy.

Olcott, P.G., 1992. Ground Water Atlas of the United States; Iowa, Michigan, Minnesots, Wisconsin. HA 730-J. <http://pubs.usgs.gov/ha/ha730/ch_j/> (accessed February 2014).

Price, M., 2009. Barometric water-level fluctuations and their measurement using vented and non-vented pressure transducers. Q. J. Eng. Geol. Hydrogen 42, 245–250. http://dx.doi.org/10.1144/1470-9236/08-084.

Quilty, E.G., Roeloffs, E.A., 1991. Removal of barometric-pressure response from water level data. J. Geophys. Res-Solid 96 (B6), 10209–10218.

Rasmussen, T.C., Crawford, L.A., 1997. Identifying and removing barometric pressure effects in confined and unconfined aquifers. Ground Water 35 (3), 502–511.

Rasmussen, T.C., Mote, T.L., 2007. Monitoring surface and subsurface water storage using confined aquifer water levels at the Savannah River Site, USA. Vadose Zone J. 6 (2), 327–335.

Ritizi, R.W., Sorooshian, S., Hsieh, P.A., 1991. The estimation of fluid flow properties from the response of water levels in wells to the combined atmospheric and Earth tide forces. Water Resour. Res. 27 (5), 883–893.

Rojstaczer, S., 1988. Determination of fluid-flow properties from the response of water levels in wells to atmospheric loading. Water Resour. Res. 24 (11), 1927–1938.

Rojstaczer, S., Riley, F.S., 1990. Response of the water level in a well to Earth tides and atmospheric loading under unconfined conditions. Water Resour. Res. 26 (8), 1803–1817.

Smedley, P.L., Neumann, I., Farrell, R., 2004. Baseline report series: 10, The Chalk Aquifer of Yorkshire and North Humberside, Rep., CR/04/128, Groundwater Systems and Water Quality, Br. Geol. Surv. Comm. Rep., NC/99/74/10, Environ. Agency Sci. Group, Keyworth, Nottingham, UK.

Spane, F.A., 2002. Considering barometric pressure in groundwater flow investigations. Water Resour. Res. 38 (6), 14-1–14-18. http://dx.doi.org/10.1029/2001wr000701.

Spane, F.A., Mackley, R.D., 2011. Removal of river-stage fluctuations from well response using multiple regression. Ground Water 49 (6), 794–807. http://dx.doi.org/10.1111/j.1745-6584.2010.00780.x.

Stuart, M.E., Chilton, P.J., Kinniburgh, D.G., Cooper, D.M., 2007. Screening for long-term trends in groundwater nitrate monitoring data. Q. J. Eng. Geol. Hydrogeol. 40, 361–376. http://dx.doi.org/10.1144/1470-9236/07-040.

Toll, N.J., Rasmussen, T.C., 2007. Removal of barometric pressure effects and Earth tides from observed water levels. Ground Water 45 (1), 101–105. http://dx.doi.org/10.1111/j.1745-6584.2006.00254.x.

Vogelsberg, A., 2007. Northern Great Plains Aquifer system. <http://academic.emporia.edu/schulmem/hydro/TERM%20PROJECTS/2007/Vogelsberg/Beryl_to_Aquifer.htm> (accessed February 2014).

Weeks, E.P., 1979. Barometric pressure fluctuations in wells tapping deep unconfined aquifers. Water Resour. Res. 15 (5), 1167–1176.

Welch, P.D., 1967. The use of fast Fourier transform for the estimation of power spectra: a method based on time averaging over short, modified periodograms. Water Resour. Res. AU-15, 70–73.

Yager, R.M., 1996. Simulated three-dimensional ground-water flow in the Lockport Group, a fractured dolomite aquifer near Niagara Falls, New York. U.S. Geological Survey Water Supply Paper 2487, p. 42.